# Structural Health Monitoring of High-speed Railway Tracks Using Diffuse Ultrasonic Wave-based Condition Contrast: Theory and Validation

**Article** *in* Smart Structures and Systems · March 2020

DOI: 10.12989/sss.2020.26.2.227

CITATIONS
5

READS
882

**8 authors**, including:

Wuxiong Cao
Harbin Institute of Technology
**30** PUBLICATIONS **164** CITATIONS

SEE PROFILE

Ye Lu
Monash University (Australia)
**89** PUBLICATIONS **3,848** CITATIONS

SEE PROFILE

**Smart Structures and Systems**, *Vol. 26, No. 2* (*2020*) *227-239*
DOI: https://doi.org/10.12989/sss.2020.26.2.227


# Structural health monitoring of high-speed railway tracks using diffuse ultrasonic wave-based condition contrast: *theory and validation*

Kai Wang [1], Wuxiong Cao [2], Zhongqing Su*[2,3,4], Pengxiang Wang [5], Xiongjie Zhang [5], Lijun Chen [5], Ruiqi Guan [6] and Ye Lu [6]

[1] *Interdisciplinary Division of Aeronautical and Aviation Engineering, The Hong Kong Polytechnic University, Kowloon, Hong Kong SAR*
[2] *Department of Mechanical Engineering, The Hong Kong Polytechnic University, Kowloon, Hong Kong SAR*
[3] *The Hong Kong Polytechnic University Shenzhen Research Institute, Shenzhen 518057, P.R. China*
[4] *National Rail Transit Electrification and Automation Engineering Technology Research Center (Hong Kong Branch), The Hong Kong Polytechnic University, Kowloon, Hong Kong SAR*
[5] *Southwest Jiaotong University Railway Development Co., Ltd., Chengdu, 610073, P.R. China*
[6] *Department of Civil Engineering, Monash University, Clayton, VIC 3800, Australia*

(*Received December 5, 2019, Revised March 24, 2020, Accepted March 28, 2020*)

**Abstract.** Despite proven effectiveness and accuracy in laboratories, the existing damage assessment based on guided ultrasonic waves (GUWs) or acoustic emission (AE) confronts challenges when extended to real-world structural health monitoring (SHM) for railway tracks. Central to the concerns are the extremely complex signal appearance due to highly dispersive and multimodal wave features, restriction on transducer installations, and severe contaminations of ambient noise. It remains a critical yet unsolved problem along with recent attempts to implement SHM in bourgeoning high-speed railway (HSR). By leveraging authors' continued endeavours, an SHM framework, based on actively generated diffuse ultrasonic waves (DUWs) and a benchmark-free condition contrast algorithm, has been developed and deployed via an all-in-one SHM system. Miniaturized lead zirconate titanate (PZT) wafers are utilized to generate and acquire DUWs in long-range railway tracks. Fatigue cracks in the tracks show unique contact behaviours under different conditions of external loads and further disturb DUW propagation. By contrast DUW propagation traits, fatigue cracks in railway tracks can be characterised quantitatively and the holistic health status of the tracks can be evaluated in a real-time manner. Compared with GUW- or AE-based methods, the DUW-driven inspection philosophy exhibits immunity to ambient noise and measurement uncertainty, less dependence on baseline signals, use of significantly reduced number of transducers, and high robustness in atrocious engineering conditions. Conformance tests are performed on HSR tracks, in which the evolution of fatigue damage is monitored continuously and quantitatively, demonstrating effectiveness, adaptability, reliability and robustness of DUW-driven SHM towards HSR applications.

**Keywords:** diffuse ultrasonic wave; structural health monitoring; high-speed railway; fatigue crack

## 1. Introduction

The integrity of railway tracks is a paramount concern in railway industry, whose significance is particularly accentuated for the burgeoning high-speed railway (HSR) in which the operational speeds of trains are 200 km/h or above. At such high speeds, any structural failure due to degraded track integrity will undoubtedly result in catastrophic consequences with miserable fatalities and immense economic loss. However, as a matter of fact, under repetitious, intensive, and heavy-duty loads, HSR tracks are highly prone to material degradation and presence of fatigue damage. Together with a variety of hazards such as atrocious climate, detrimental impacts, complex rail conditions, unexpected events including sabotage, such degradation and fatigue damage impose vast threat to the integrity and safety of HSR rails. Without timely awareness and appropriate remedial actions, embryonic fatigue damage can deteriorate to a critical level at an alarming rate without sufficient warning. Exemplarily, on November 20, 2016, the fatigue-induced fracture in a railway track caused a train derailment at Kanpur, India, resulting in at least 150 dead and another 150 injured (2016).

The importance of warranting the integrity of HSR tracks, and in particular for key sections such as railway switches and turnouts, cannot be over-emphasized, which has entailed numerous non-destructive evaluation (NDE) techniques (Ghiasia and Ghasemi 2018, Han *et al*. 2014, He *et al*. 2018, Ph Papaelias *et al*. 2008, Wang *et al*. 2019a, Zhang *et al*. 2015) that have been tailor-made for HSR and well commercialized. Prevailing NDE techniques available for rail maintenance are represented by those using eddy current (Rajamäki *et al*. 2018, Song *et al*. 2011), visual cameras (Mair and Fararooy 1998), magnetic testing (Liu *et al*. 2015, Santa-aho *et al*. 2014), and ultrasonic inspection (Bartoli *et al*. 2005, Rao *et al*. 2016, Wang *et al*. 2019b, 2015, Zuo *et al*. 2016) to name a few. Central to the interest is the ultrasonic inspection, and Fig. 1 shows two representative mobile ultrasonic inspection devices in which

*Corresponding author, Professor,
E-mail: Zhongqing.Su@polyu.edu.hk



ISSN: 1738-1584 (Print), 1738-1991 (Online)


Fig. 1 Commercialized mobile ultrasonic inspection devices for detecting damage in railway tracks: (a) portable rail detector (Clark 2004); and (b) air-coupled ultrasound transducer-based detection vehicle (Mariani *et al*. 2017)

portable ultrasound transducers are manipulated respectively by a walking operator and by a slowly moving vehicle, for detecting damage in railway tracks.

Nevertheless, today's prevailing NDE techniques for railway track inspection and maintenance are either manoeuvred with a vehicle or by a sophisticated operator, performed at regularly scheduled intervals after terminating normal operation of the railway system. Time-consuming, labour-intensive and cost-exorbitant, these techniques fail to evaluate the overall status of a long-range track promptly and cost-effectively, and they are unwieldy for timely awareness of fatigue damage at its initial stage. Moreover, owing to the strict restriction on transducer installation onto railway tracks, the detectable region is limited to the rail head and web only, possibly overlooking damage in rail foots.

To circumvent these deficiencies of conventional NDE techniques when applied to real HSR industry, emerging structural health monitoring (SHM) has been intensively explored, with an aim of providing continuous and automated surveillance of the health condition of railway tracks in a near real-time manner (Adams 2007, Bao *et al*. 2013). With integrated transducers, fast signal processing and autonomous operation, material degradation, structural damage and overall health status of the tracks can be monitored *in situ* and continuously. Effective and precise monitoring further enables prognosis of track failure and system breakdown. In particular, the acoustic emission (AE) signals, captured by fibre Bragg gratings (FBG) sensors or lead zirconate titanate (PZT) sensors when damage initiates or deteriorates under external loads induced by the train passage or thermal loads, are used to locate the damage in rails (Thakkar *et al*. 2006, Wang *et al*. 2018, Zhang *et al*. 2018a). Despite that some AE-based SHM systems have already been commercialized and installed on railroads, this category of techniques may show inferior fidelity, reliability, adaptability and environment-tolerance when compared with active measurement-based inspection. That is mainly attributable to the fact that AE signals, passively acquired in uncontrollable conditions, are highly prone to contaminations from ambient noise including ambient fluctuation and running vehicles, which can trigger false-positive alarm and in the meantime mask the signal changes induced by the presence of fatigue damage.

In lieu of passive AE-based methods, alternative approaches using actively generated guided ultrasonic waves (GUWs) have been increasingly preferred. The interaction between GUWs excited at desired frequencies and damage in tracks induces wave scattering, wave reflection or transmission, energy dissipation, mode conversion and other subtle wave features (Cawley *et al*. 2003, Lanza di Scalea *et al*. 2005, Li *et al*. 2009, Su *et al*. 2014). By perceiving and calibrating changes in these wave features against baseline signals acquired from intact counterpart structures, diverse damage indices are constructed and linked to different damage parameters such as location, size, and severity. GUW-based inspection usually presents enhanced immunity to ambient noise and measurement uncertainties when compared against the passive AE-based approaches. However, when extended to railway tracks, GUWs-based inspection still confronts vast challenges, mainly including the extremely complex wave signals (as a result of multimodal and dispersive features of GUWs), perplexing wave scattering/reflections at irregular boundaries of rail structures, and drift of baseline signals caused by service condition fluctuation. Together, these factors lead to difficulty in GUW feature extraction and signal interpretation, precluding GUWs-based methods from delivering accurate assessment of the health status of railway tracks.

Motivated by the recognition of unsatisfactory performance of both the passive AE-based and active GUW-based SHM in HSR industry, a diffuse ultrasonic waves (DUWs)-driven damage evaluation philosophy and a SHM framework are developed, by leveraging the diffused natures of DUWs and their superb characteristics including convenience in signal actuation and acquisition, long-range reachability and adaptability (Chen *et al*. 2012, Croxford *et al*. 2016, Michaels and Michaels 2005, Shen and Cesnik 2018, Zhang *et al*. 2017). DUWs disseminate in the entire railway track quickly and adequately, from which rich information can be extracted upon appropriate processing for accurate evaluation of the overall health of the railway track. To facilitate implementation of DUW-based SHM in real HSR and minimize the dependence of monitoring on baseline signals, a benchmark-free condition-contrast algorithm is developed, via which the unique patterns manifested by DUWs diffused in railway tracks bearing fatigue cracks, under different conditions of external loads, are differentiated. On this basis, a set of damage indices is constructed and associated with the accumulative severity and growth of fatigue cracks in the railway tracks, from a microscopic to a macroscopic level. Continuous monitoring further enables real-time awareness of the integrity of railway tracks under inspection. The proposed SHM framework is deployed via a self-configured all-in-one SHM system in conjunction with a sparse piezoelectric sensor network. The approach and system are validated in conformance tests, in which the deterioration of a fatigue

crack in a railway track acquired from China's HSR is continuously monitored. Results have proven that the developed SHM framework has, to a certain degree, ushered a new avenue to cost-effective SHM approaches capable of accommodating real-world applications in HSR industry.

## 2. Principle of DUW-driven SHM for railway tracks

The railway track, *per se*, is of a complex waveguide, in which ultrasonic waves are multi-scattered by boundaries in the cross section of the rail and the acoustic energy is rapidly reverberated, and analogous to a diffusive medium, this leads to the generation of multiple random propagation paths and a highly diffused wavefield. Such a diffused yet stable wavefield is referred to as *diffuse ultrasonic wave* (DUW). Though complex in appearance, diffuse waves are fairly repeatable yet sensitive to perturbation in the waveguide (e.g., a flaw). By treating it as a hostile feature, DUW renders the possibility to accurately detect changes, even subtle, in material or structural properties of railway tracks. As a representative modality of diffuse waves, the coda waves, widely used for seismogram analysis in geosciences, have been proven effective in structural damage identification, even when the change is insignificant such as that caused by undersized damage, external loads or ambient fluctuation (Hilloulin *et al*. 2014, Larose *et al*. 2010, Planès and Larose 2013, Zhang *et al*. 2018b). Despite their noisy and chaotic appearance, coda wavefields are favorably stable and repeatable, so that the waveforms are identical if no change occurs in the waveguide over the time; in contrast, if perturbation occurs (e.g., the presence of a crack in the waveguide), phenomenal changes can be observed in the wavefields. Even though, the use of DUWs for SHM of rail structures is hitherto fairly rare and limited, which might be attributed to inadequate understanding of the propagation characteristics of DUWs in rail structures, along with a number of technical challenges during practical implementation such as wiring and cabling for actuators/sensors, real-time signal acquisition, and processing of massive signals.

The diffusion of acoustic energy emitted by an ultrasonic transducer into the railway track – a diffusive medium, can be depicted using the one-dimensional diffusion equation with dissipation (Anugonda *et al*. 2001), which reads

$$D\frac{\partial^2}{\partial z^2}\big(E(z,t)\big)-\frac{\partial}{\partial t}\big(E(z,t)\big)-\sigma\big(E(z,t)\big) = E_0\delta(t)\delta(z), \tag{1}$$

where $D$ is the acoustic diffusivity, and $\sigma$ the dissipation. $t$ is the time. $E_0$ denotes the incident energy which is excited at $z=0$ at time $t=0$ (see Fig. 2). $\delta$ is the Dirac delta function. With Eq. (1), the evolution of the ensemble average energy density $E$ can be calculated.

Allowing for the strict limitation of instrument installation on railway tracks, only two miniaturized PZT wafers are utilized in the approach to form a highly sparse sensor network, one for generation of DUWs in a long range railway track and the other for DUW acquisition, as illustrated schematically in Fig. 2. With this sparse sensor network, incident waves are excited and emitted into the track, and after multiple reverberation and mode conversion in the track, a multitude of wave modes form a stable DUW wavefield, encompassing longitudinal waves, shear waves, surface waves and guided waves. To ensure that all these modalities of wave modes are included in a captured signal, the DUW wavefield shall be recorded in a sufficiently long period.

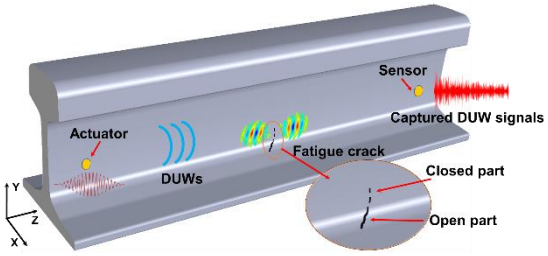


Fig. 2 Schematic of DUW generation and acquisition in a railway track

The premise of the proposed DUW-driven SHM lies in a fact that the damage in a waveguide, if any, can distort DUW propagation and deviate wave features from those of baseline signals that are pre-collected from an intact counterpart. By contrasting the captured DUW signals against baseline signals, the damage can be identified and characterized. However, it usually takes an extended period for a new railway track in service to witness initiation of fatigue damage and subsequent damage progressing. Prior to initiation of fatigue damage that is worthy of being concerned, the ambient factors such as the instability (even error) of measurement system, aging of instruments and devices, and time varying service conditions (e.g., temperature variation) may lead to changes in baseline signals even without the presence of any structural damage. Moreover, the changes in ambient factors can overwhelm those induced by embryonic damage such as a fatigue crack. This implies that the baseline signal which is pre-acquired from an intact counterpart under specific measurement conditions, can vary against time, even without the presence of damage, leading to outdated benchmark and therefore eroding confidence in the evaluation results. Against this backdrop, a condition contrast method is proposed, to supplement the DUW-driven SHM, which contrasts DUW signals captured from a railway track under different loading conditions. With the condition contrast, a baseline signal from the intact railway track is no longer of necessity, whereby to minimize the dependence of monitoring on baseline signals.

Limiting the concerned damage type to fatigue cracks in railway tracks, this section briefly discusses the theory, principle, and methodology of the proposed SHM framework.

### *2.1 Crack opening/closure vs. load conditions*

Under an external load, the fatigue cracks in railway tracks can be initiated and progressively developed. These

fatigue cracks can be manifested in different parts of a railway track: on the rail head under the cyclic wheel/rail contact stress, at the rail foot due to corrosion pits, at holes or cuts where stress is concentrated, or at the weld at which imperfection and defect (e.g., porosity, shrinkage stress and impurity) exist. Naturally, the two surfaces of a fatigue crack are in contact under most circumstances in the vicinity of the crack tip, owing to the crack closure phenomenon induced by the plasticity, residual stress or by oxide films ("closed part") (Buck *et al*. 1988, Pippan and Hohenwarter 2017), while the rest part of the crack is of an air gap between the two surfaces ("open part"), as illuminated schematically in the insert of Fig. 2.

It is commonly known that an open crack – similar to a void, induces disturbance in wave propagation, causing wave scattering and mode conversions, while a closed crack leads to inconspicuous distortion in wave features. Under external loads (e.g., a three-point bending load or a tensile load), the status of the crack alternates to be closed or open (Ohara *et al*. 2011, 2007). Therefore, the alternation of the crack contacting status (open or closed) under external loads can modulate DUW propagation and deviate wave features from those under a load-free condition. Making use of such a principle, a fatigue crack can be identified and characterized, which serves as the cornerstone of the proposed SHM framework.

### 2.2 Benchmark-free condition contrast

In the proposed SHM framework, DUWs propagating in a railway track, regardless of presence of fatigue damage, are captured in two separate conditions in tandem: (i) when the track is load-free; and (ii) when the track is subjected to an external load (e.g., a moving train). Changes in the contacting status of a crack, if present, can be triggered as detailed in the preceding section, to further modulate DUWs. Usually, acquisition of DUW signals in both conditions in tandem can be performed instantaneously (within seconds), and during the whole process the system, instrument, and environment can be confidently deemed unchanged, and this makes the proposed method immune to the thermal drift, environment noise, and system errors, without which the damage-induced changes in DUW features can be precisely extracted, conducive to remarkable enhancement of monitoring robustness.

### 2.3 Damage indices (DIs)

Upon acquisition of DUW signals, a set of four damage indices (DIs hereinafter) is defined, mutually supplementing to each other for improvement of monitoring precision and robustness. Four DIs link different DUW features (e.g., de-correlation of DUWs and relative change in wave propagation velocity) to particular damage parameters such as crack location and severity, serving as sensitive indicators to alert the presence of fatigue crack and benefit accurate evaluation of the overall health status of the railway track under inspection.

#### 2.3.1 De-correlation-based DI

Knowing the gap between two neighbouring track sleepers, a typical load that is exerted on the railway track by a moving train can be equivalent to a three-point bending, as illustrated schematically in Fig. 3. When an external load causes a tensile stress at the crack, part of the closed crack tends to open and further disturb DUWs. The higher a tensile load, the larger proportion of the opened crack will be. On top of that, an external load can also expedite fatigue crack progress, and intensify the changes in DUW features.

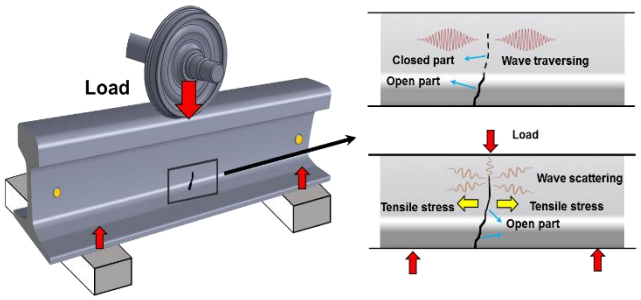


Fig. 3 Load-induced alternation of contacting status of a fatigue crack in a rail track and consequent variation in traversing DUWs

The first genre of DI is proposed, based on the de-correlation between two DUW signals, respectively captured from a loaded condition and a load-free condition, to quantify the crack-induced perturbation in DUW propagation. Let $X(t)$ be the DUW signal acquired in a load-free condition, and $Y(t)$ from the rail under a loaded condition. The remnant correlation coefficient (RCC), which is a normalized coefficient indicating the level of de-correlation between DUW signals $X(t)$ and $Y(t)$ (from 0 to 100%), is defined as

$$RCC = 1 - \frac{\int X(t)\cdot Y(t)\,dt}{\sqrt{\int X(t)^2\,dt \cdot \int Y(t)^2\,dt}}. \tag{2}$$

$RCC$ is related to the crack severity, according to the illustration in preceding section.

#### 2.3.2 Local temporal correlation-based DI

Considering the highly complex waveform of a DUW signal, the second genre of DI is proposed, in virtue of the signal local correlation coefficient (LCC) in the time domain, which quantifies the local correlation between two time-series signals $X(t)$ and $Y(t)$, is defined as

$$LCC^{(t)}(\tau) = \frac{\int_{t-T}^{t+T} X(s)\cdot Y(s+\tau)\,ds}{\sqrt{\int_{t-T}^{t+T} X(s)^2 ds \cdot \int_{t_1}^{t_2} Y(s+\tau)^2 ds}}. \tag{3}$$

Eq. (3) provides an amplitude-independent measure of the similarity in the waveform of two DUW signals within a time window [t-T, t+T] when the second signal is delayed by $\tau$ from the first. Different from $RCC$, $LCC^{(t)}$ accentuates the localized nature of the coherence between two DUW signals, because part of, rather than entire of, the wave packet of a DUW signal, under the modulation of a fatigue crack, changes more remarkably than the rest. In accordance with Eq. (3), a parameter $PC(t)$ is further

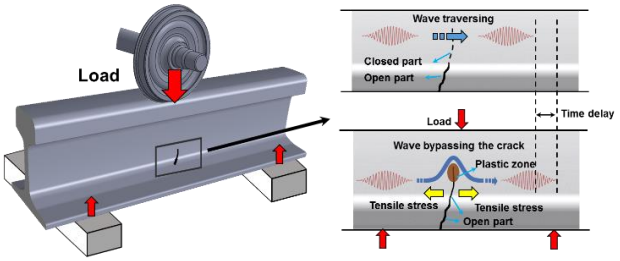


Fig. 4 Load-induced alternation of contacting status of a fatigue crack in a rail track and consequent time delay in wave propagation due to a reduced propagation velocity

defined, which is the peak of the absolute value of $LCC^{(t)}$ with respect to the delay $\tau$ at each moment $t$, and it reads

$$PC(t) = \max_{\tau}\left(LCC^{(t)}(\tau)\right). \quad (4)$$

Similarly, a local remnant correlation coefficient ($LRCC(t)$) is defined to measure the fatigue crack-induced local changes in DUW signals, as

$$LRCC(t) = 1 - PC(t). \quad (5)$$

### 2.3.3 Velocity change-based DI

As discussed earlier, the opening of the crack from a closed status caused by the load can block wave transmission through the crack. At a partially open crack, the incident waves bypass the two crack surfaces and crack tips, leading to a certain degree of time delay, compared with wave propagation in a load-free condition, as illustrated in Fig. 4. In addition, the load induces plastic deformation at the crack tips that lowers the local elastic modulus and decreases the propagation velocity of transmitted waves.

A signal stretching manipulation (Hilloulin *et al*. 2014, Lobkis and Weaver 2003) is recalled, by assuming that the variation in propagation velocity of DUW under a loaded condition will result in either compression or stretching of signal $Y(t)$ with regard to a reference signal, $X(t)$, that is acquired from the scenario in which DUW propagates under a load-free condition. To reflect such variation in the propagation velocity of acoustic energy, the third DI is constructed, based on the correlation between the stretched signal $X(t(1+\xi))$ from a load-free condition and the signal $Y(t)$ from a loaded condition, as

$$SC(\xi) = \frac{\int X(t(1+\xi)) \cdot Y(t)\, dt}{\sqrt{\int X(t(1+\xi))^2 dt \cdot \int Y(t)^2 dt}}. \quad (6)$$

In Eq. (6), when $SC(\xi)$ reaches its maximum, the corresponding $\xi$ is denoted as $\bar{\xi}$ which represents the relative stretching degree in the arrival time of the acoustic energy. Therefore, $\bar{\xi}$ signifies the relative variation in the propagation velocity, and $\bar{\xi} = \frac{V_1 - V_0}{V_0}$, in which $V_1$ and $V_0$ represent the propagation velocity of waves from a loaded and load-free condition, respectively.

### 2.3.4 Local velocity-based DI

Addressing the localized nature of a fatigue crack, the fourth DI is constructed by extending Eq. (3) which reflects the effect of fatigue crack on propagation velocity of individual wave modes in DUWs. When $LCC^{(t)}$ in Eq. (3) reaches its peak $PC(t)$ at moment $t$, the corresponding delay $\tau$ is denoted as $\bar{\tau}$, and it reads

$$\bar{\tau}(t) = \arg\max_{\tau}\left(LCC^{(t)}(\tau)\right). \quad (7)$$

$\bar{\tau}(t)$ measures the local time delay of the DUW signal $Y(t)$ from $X(t)$ within a time window $[t\text{-}T, t\text{+}T]$. Because the velocity variation is correlated with the change of material properties of the track (such as occurrence of fatigue damage), the defined coefficients $\bar{\xi}$ and $\bar{\tau}(t)$ can be used as indicators of damage.

## 3. Development of system and sensors

Distinct from laboratorial measurement in which DUW generation and acquisition can be easily achieved with isolated devices and instruments such as wedge probes, function generators and signal processing unit, the *in* situ implementation of an SHM framework in real-world applications desires an integrated system with all functional

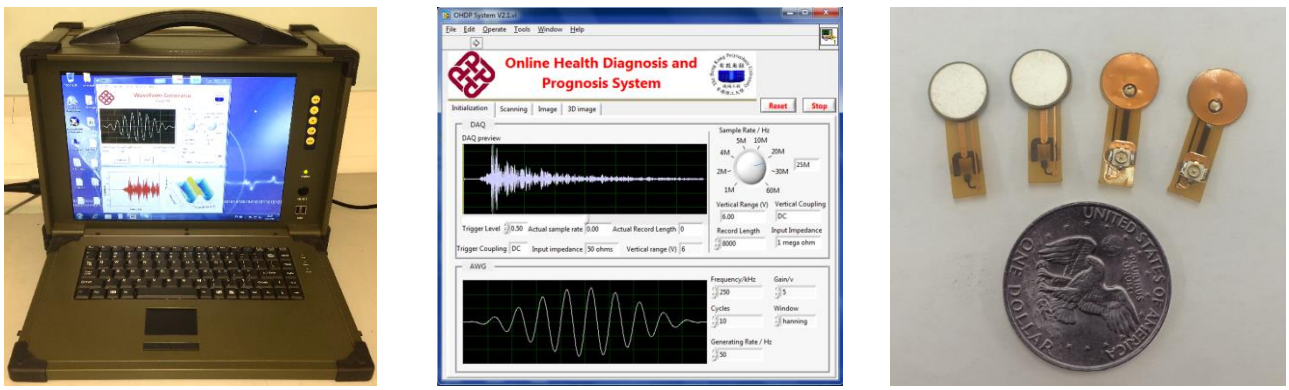


(a) (b) (c)

Fig. 5 (a) All-in-one system for in situ implementing DUW-driven SHM, wave generation and signal acquisition modules are included; (b) software interface of the system; (c) miniature and flexible PZT wafer-based sensors

units embedded in the system via a communication bus. To implement the proposed DUW-driven SHM framework in real-world railway industry, an all-in-one system is designed and manufactured, with its final assembly pictured in Fig. 5(a). The system, based on a PCI extension for Instrumentation (PXI) platform with the virtual instrument technique, embraces mainly an arbitrary wave generation module (with high-power amplification), a multi-channel data acquisition module, and a central control and data processing module. An in-house software package is programmed on NI® LabVIEW platform, Fig. 5(b), for the controlling of individual modules and post-processing of DUW signals, via which DUW generation, signal acquisition and railway track integrity evaluation can be fulfilled. The system fully accommodates the needs of automatic and online SHM for rails.

Considering practical requirements of fulfilling *in situ* acquisition of DUWs, miniaturised PZT wafers are selected, due to their salient merits including substantial weight saving over conventional ultrasound transducers, flexibly customised footprints, ease integration with rail structures, broad response frequency range, a dual-role as both wave actuator and sensor, as well as low cost. A sparse sensor network, with the use of only two distributed PZT wafers, is sufficient to perform the DUW generation and acquisition, enabling *in situ* implementation of developed SHM framework economically and conveniently. Different from GUW-based approaches in which the locations of individual transducers have to be selected prudently so as to avoid complex boundary reflection, DUW-drive SHM does not entail an exhaustively prudent selection of the positions of individual sensors, because interpretation of individual wave components of a DUW signal including complex boundary reflection is not of necessity. It is such a trait that makes it possible to evaluate the health status of various rail components such as the railway switches or turnouts which feature highly complex geometries. It is envisaged that to manually immobilise individual sensors on railway tracks using adhesives and to solder shielded cables on each of them unavoidably jeopardize the consistency of DUW acquisition among sensors.

To circumvent this, a standardized sensing unit, pictured in Fig. 5(c), is designed and fabricated. Each sensing unit embraces a PZT wafer (PI®, P51, diameter: 12 mm and thickness: 1 mm) and two associated electrodes, all of which are encapsulated in a thin polyimide film. Thin, flexible and to be permanently mounted on a railway track, the polyimide film is readily adaptive to the curvature of non-flat parts of the track. To ensure its functionality in rugged working conditions, each sensing unit is insulated from the environment via a thin layer of epoxy after immobilised on the rail (to be detailed in Section 4.1). In-field tests prove that such protection can greatly enhance the survivability of sensing units in atrocious operation conditions of HSR.

## 4. Experimental validation

Aimed at proof-of-concept, conformance tests were accomplished, in which the health status of a railway track was monitored using the developed SHM framework and configured all-in-one system. The selected railway track section, made of high-strength steel (GB2585-2007 P60 kg), measuring 1.2 m in length, is part of the HSR network in China supporting passage of trains traveling at a speed up to 380 km/h.

### *4.1 Experimental set-up*

As commented earlier, only a pair of the designed PZT sensing units, making use of the dual roles as an actuator and a sensor for each, can warrant the generation and acquisition of DUWs to inspect a long range of the track. Such a pair of sensing units (denoted by PZT1, PZT2) was surface-mounted on the ends of the railway track, as seen in Fig. 6(a). One of the units was on the left side (100 mm from the left end of the track) and the other on the right side (100 mm from the right end). Restricted by the codes of safe operation of HSR, the sensing units were located at the rail web, 70 mm high from the rail bottom. Each unit, upon installation and before wiring, was thoroughly protected by a thin layer of epoxy coating and then instrumented with the all-in-one system.

Considering the loads applied on the track from a train, a three-point bending test was performed on the railway

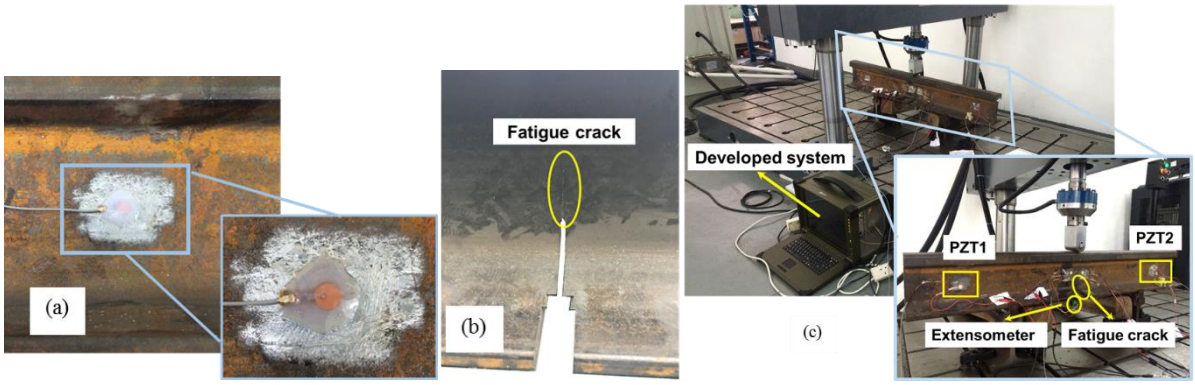


Fig. 6 (a) A sensing unit sensor installed on the railway track capsulated with a thin layer of epoxy coating; (b) a notch in the railway track serving as crack precursor and a fatigue crack initiated from the notch tip after fatigue tests; (c) set-up of conformance tests

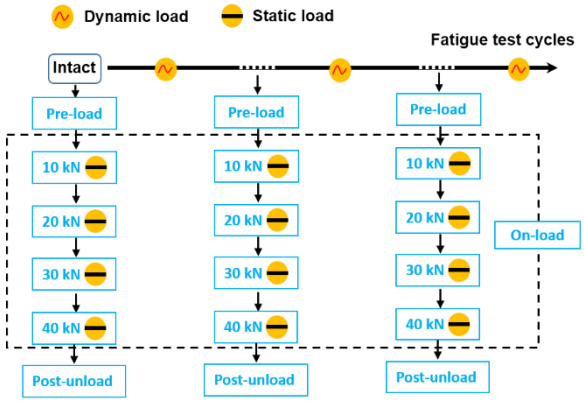


Fig. 7 DUW test flowchart in conformance test: the fatigue test was suspended after every 18,000 cycles, and during each pause, the DUW tests were performed at three sequent loading states

track. The two supporting points were positioned with the distance of 0.6 m which was consistent with the reality of HSR – the gap between two sleepers. Considering the weight of a typical high-speed train coach in real world (45,000~60,000 kg), a cyclic load (10~50 kN) with a frequency of 10 Hz was applied at the midpoint of the upper surface of the railway track through a fatigue test machine (ENPUDA®). In reality, it takes an extended period to witness the initiation and progress of fatigue damage in railway tracks. In this experimental validation, to shorten such a period, a notch was pre-machined at the midpoint of track bottom to serve as a crack precursor. After ~108,000 cycles of fatigue load, a fatigue crack, measuring 30 mm in length, was generated from the notch tip, as displayed in Fig. 6(b). An extensometer was mounted on the notch to monitor the crack opening under tensile stress, Fig. 6(c), via which the severity of the fatigue crack can be assessed in a real-time manner.

The fatigue test was suspended after every 18,000 cycles. During each pause, the DUW tests were performed, in which the DUW was generated using the PZT wafer on the left and captured with the other on the right side, at three sequent loading states, with a working flowchart illustrated in Fig. 7:

(i) before application of any load – the *pre-load condition*;
(ii) during application of a static load increasing from 0 to 40 kN with an increment of 10 kN – the *on-load condition*; and
(iii) after removal of the static load – the *post-unload condition*.

In the DUW test, ten-cycle narrow band sinusoidal tone bursts modulated by a *Hanning* window and within a working frequency band of 200~800 kHz were excited by the waveform generation module of the all-in-one system as the input signal. Frequency tuning (Hong *et al*. 2014) was implemented to select the most optimal frequencies in the working frequency band, to determine 250 kHz as the excitation frequency in all the tests, at which the strongest responses of generated DUW was observed, implying the highest signal-to-noise ratio. The input signal was applied on the PZT wafer functioning as the DUW wave generator. Given a propagation velocity of ~5 km/s of the longitudinal wave mode in the selected railway track, the incident wave energy can be diffused sufficiently within a time span of 10 ms, and therefore DUW signals in a period of 10 ms were collected at a sampling rate of 25 MHz through the data acquisition module of the system. The collected data from consecutive 128 scans were averaged to eliminate measurement uncertainties.

Subsequently, DUW features were extracted from captured DUW signals to establish the proposed DIs using Eqs. (2)-(7). With DIs, the accumulative severity of the fatigue crack was evaluated, and its progress was monitored continuously.

### *4.2 Evaluation of crack severity*

To begin with, the crack opening displacement (COD) obtained from the extensometer is displayed in Fig. 8. It clearly shows that the progress of a fatigue crack embraces two main stages: fatigue crack initiation and rapid propagation. In the former stage, the COD increases with the fatigue cycles at a steady rate, whilst in the later stage a much higher rate for the COD increasing is observed. The relatively steady increase of COD in the former stage can be attributed to the growth of micro-crack and the plasticity in the railway track, particularly at the notch tip where the stress concentration is prominent. Upon formation of a macroscopic crack with a certain gap between the two crack surfaces in a later stage, the rapid propagation of the crack triggers a fast increase in COD.

To evaluate the accumulative crack severity, DUW signals from the pre-load and on-load conditions are contrasted, to leverage a load-induced alternation of the contacting status of the crack as detailed in Section 2.1. The DUW signals, acquired when the track was intact and after 108,000 fatigue cycles applied, are shown in Fig. 9. Highly intricate, a DUW signal comprises numerous wave packets that are overlapped and intertwined with others, making it challenging to discern individual wave modes and interpret wave propagation if conventional GUW-based methods used.

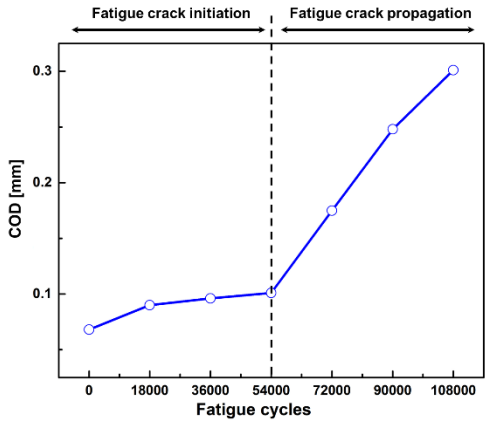


Fig. 8 Relation between COD and fatigue cycle in tests

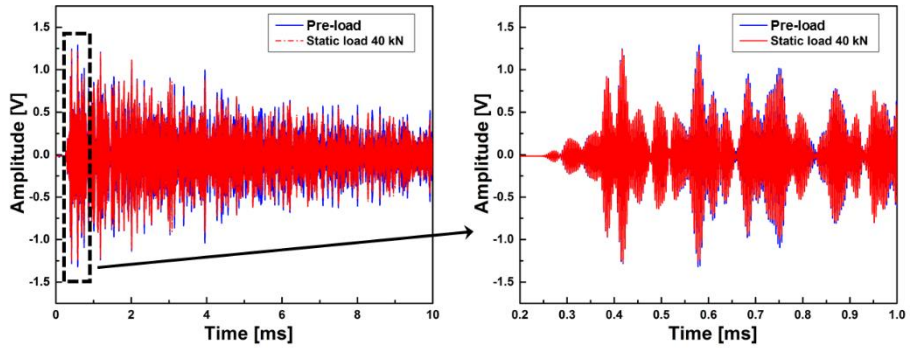


(a)

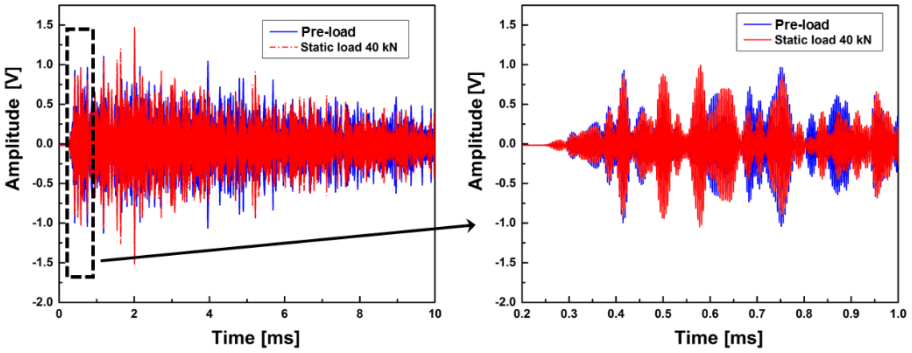


(b)

Fig. 9 (a) DUW signals acquired from the intact railway track: the difference between the signals from pre-load and on-load conditions is insidious; (b) DUW signals acquired from the track after 108,000 fatigue cycles: the difference between the signals from pre-load and on-load conditions is remarkable

From the DUW perspective, it is noted that in the intact state (Fig. 9(a)), the DUW signal when the railway track is subjected to a 40 kN load is deviated slightly from that in a pre-load condition. On the contrary, for the damaged state (with a crack length of 30 mm), a conspicuous discrepancy is manifested as displayed in Fig. 9(b). The slight deviation in the Fig. 9(a) can be caused by the influence of wheel on the wave propagation in the rail, considering that the waves can propagate from the rail to wheel and vice versa via the connection formed between the wheel and rail due to the load. Using Eq. (2), the *RCC* of DUW signals from different load conditions can be ascertained, as shown in Fig. 10. Fig. 11 asserts that the *RCC* share a common trend in variation with that of the COD: a steady increase in the first stage, followed with a rapid increase in the second stage. Also observed in Fig. 10, a higher load applied on the railway track leads to a larger opening portion of the crack which further alternates the contacting status and gives rise to a greater *RCC*. It is interesting to observe that at ~36,000 fatigue cycles all curves manifest an abnormal increase, as circled in Fig. 10, breaking the monotonic increase of the relationship between *RCC* and fatigue cycles. Such abnormality can be attributed to the fact that the applied static load drives the fatigue crack to propagate, which induces additional variation in wave scattering besides the load-induced alternation of contacting status of the crack.

As analysed in Section 2.3, the growth of micro-crack in the railway track leads to a steady increase of *RCC* in the former stage, and upon the formation of a macroscopic crack in the later stage, the rapid propagation of the

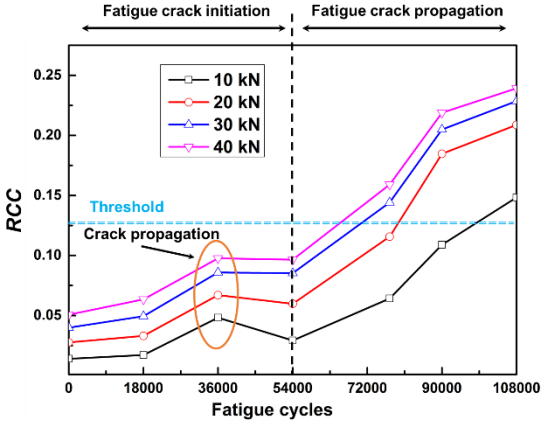


Fig. 10 RCC of DUW signals acquired when the railway track free of load and subjected to static loads

crack causes the fast increase in the closed crack and a higher increasing rate of the *RCC*. Based on this phenomenon, the *RCC* and its increasing rate can be used as an indicator to assess the evolution of the fatigue damage, and more importantly, to provide a prognosis of the fracture which is not of enough warning.

Using Eq. (3), the *LCC* can be ascertained and Fig. 11 displays the *LCC* (pre-load *vs.* on-load of 40 kN) obtained from the intact state and damaged state (with a crack length of 30 mm), from which *LRCC* can further be calculated using Eq. (5), in Fig. 12(a). Compared with the intact case, the *LRCC* from the damaged state augments holistically

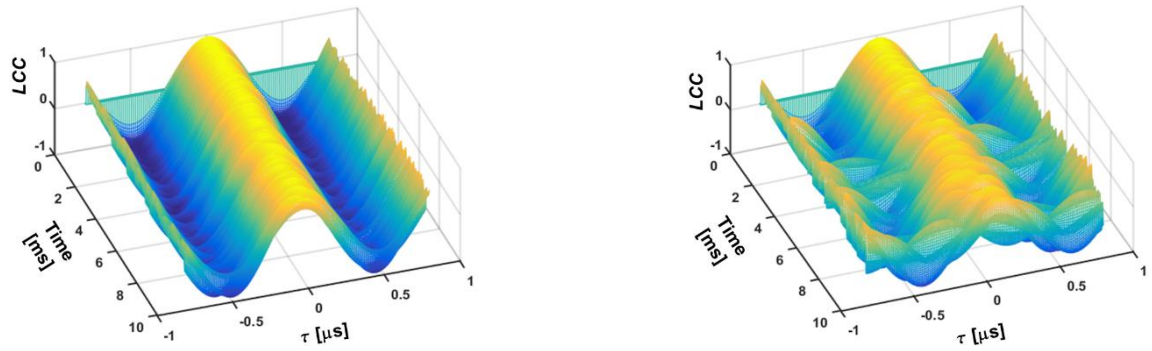


(a) (b)

Fig. 11 LCC of DUW signals obtained when the railway track subjected to a static load and load-free: (a) in intact status; and (b) after 108,000 cycles of fatigue load

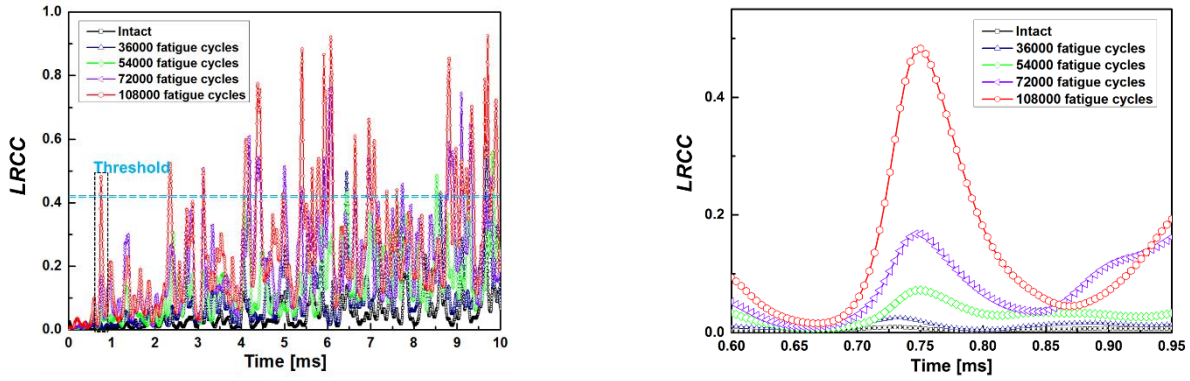


(a) (b)

Fig. 12 (a) LRCC obtained after different cycles of fatigue load; and (b) zoomed-in LRCC in a local temporal window in (a)

with fatigue cycles, and at specific local temporal windows the increase in *LRCC* is remarkable, with one example shown in Fig. 12(b). This remarkable increase originates from the localized nature of the fatigue crack in the track, as interpreted in section 2.3, and the severer the damage the more remarkable the increase in *LRCC* will be.

To shed light on the effect of the presence of fatigue crack on DUW propagation velocity, Fig. 13 compares the raw DUW signals acquired from the intact track and from the damaged case (with a crack length of 30 mm), to observe that in the intact case the phase of DUW is advanced when subjected to a static load, against the counterpart signal in a pre-load condition. On the contrary, with presence of a fatigue crack in the track, the delay of the DUW phase is induced when the track is subjected to a static load, this decreasing the stretching coefficient $\bar{\xi}$ as defined by Eq. (6). In accordance with Eq. (6), the stretching coefficient $\bar{\xi}$ is obtained and shown in Fig. 14, to note that $\bar{\xi}$ decreases from a positive in an intact case to a negative in a damaged case. The interpretation of this phenomena is that in an intact track, the elastic modulus of the track is influenced by the load due to the acousto-elasticity of the steel; with higher cycles of fatigue load, the fatigue crack which embraces the closed and open parts deteriorates at the notch, and when subjected to a load which induces a tensile stress to the crack, the waves traversing at the closed part of the crack are disturbed (as detailed in Section 2.4), and this leads to the delay of the arrival of DUWs at the sensor, causing decrease in the stretching coefficient$\bar{\xi}$. Earlier studies (Adler *et al.* 1986, Gandhi *et al.* 2012) have also corroborated such interpretation, in which the velocity change due to the stress and the velocity reduction induced by the wave scattering at the crack are experimentally demonstrated. It is noteworthy that the influence of the wheel on the wave propagation in the rail can also contribute to the deviation shown in Fig. 13(a). Analogous to *RCC*, an abnormal decrease in $\bar{\xi}$ at 36,000 fatigue cycles is exhibited, as circled in Fig. 14, which is caused by the crack propagation induced by the applied load.

Using Eq. (7), the local time delay $\bar{\tau}(t)$ obtained when the railway track is subjected to a 40 kN load, in Fig. 15, unveils a trend that is similar to that of $\bar{\xi}$: (i) in the intact state the wave phase advancing can be triggered by an applied load, and the higher the load the greater the degree of advancing it will be; (ii) in the damaged state the advancing induced by the load tends to decrease; and (iii) as fatigue damage progresses to a certain degree, the delay of the arrival time of DUW will be incurred when the track is subjected to a load. These results agree well with the theoretical analysis as detailed in Section 2.3, validating that the $\bar{\tau}(t)$ can be used to indicate the presence of fatigue damage in the railway track and further evaluate its severity.

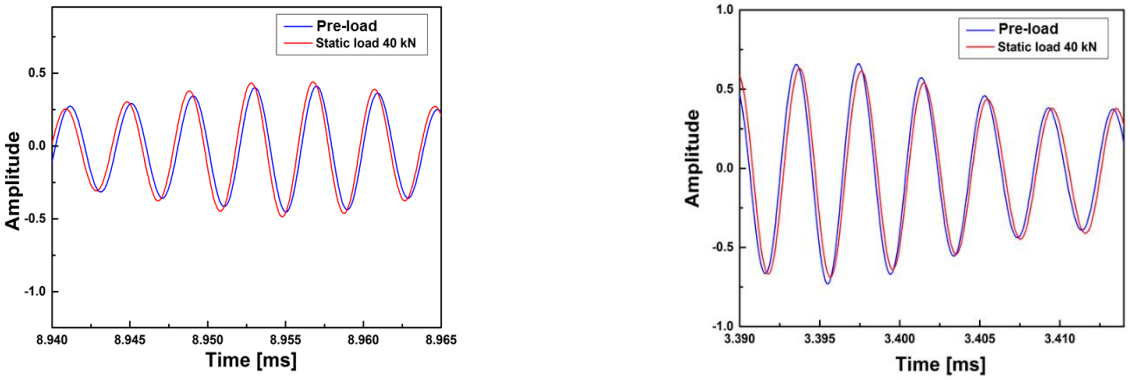


Fig. 13 DUW signals obtained from the railway track: (a) in the intact state; and (b) in the damaged case (with a crack length of 30 mm)

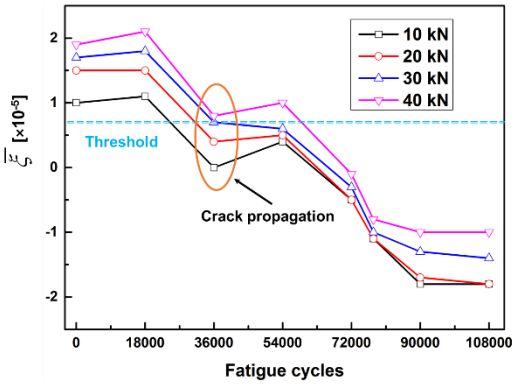


Fig. 14 Stretching coefficient obtained at different fatigue cycles and under different degrees of load applied on the track

The above results have proven that all the proposed DIs (*RCC* (Eq. (2)), *LRCC* (Eq. (5)), $\bar{\xi}$ (Eq. (6)), $\bar{\tau}$ (Eq. (7))) are monotonically linked to the crack severity, and therefore can be inversely used to evaluate the accumulative severity of a fatigue crack in the railway track. Provided respective thresholds for the the proposed DIs are set and met the maintenance can be alarmed.

### *4.3 Deteection of crack propagation*

Taking a step further, the developed SHM framework and system were also validated by monitoring the continuous progress of a fatigue crack in the railway track under a low-cycle fatigue load or a static load. When subjected to a static load, the crack propagation can be induced, generating acoustic emission and introducing changes in the railway track. It is well noted that the severer a fatigue crack, the higher probability of the crack propagation will be. To identify the crack propagation, if any, caused by the load, the contrasting between the DUW signals acquired in a pre-load condition and that obtained in a post-unload condition is utilized.

Using Eqs. (2)-(7), the proposed four DIs were ascertained, as shown in Fig. 16. From these DIs, it is clear that the four DIs (*RCC, LRCC,* $\bar{\xi}$and $\bar{\tau}$) (of the signals acquired from pre-load and post-unload conditions) extracted from DUWs at 36,000 fatigue cycles are most remarkable, arguing that crack propagation is induced by the static load at 36,000 fatigue cycles. The crack propagation induced by the static load in the DUW test provides the interpretation of the abnormal increase in the *RCC* and decrease in $\bar{\xi}$ as previously observed in Figs. 10 and 14.

It is worth noting that the length of the continuously welded rail, which is widely used in railway industries, does not impair the effectiveness of the proposed method, considering that the defect alters the propagation of traversing waves in a similar manner regardless of the length of the track. In reality, the train passage can lead to the vibration of the rail track, causing changes in the ultrasonic wave signals. Nevertheless, the vibrations induced by the passing train are usually at a frequency which is much lower than that of the probing waves, and thus the vibration-induced disturbance can be eliminated with an appropriate high-pass filter. In addition, the damage indices obtained using the signals acquired before and after the train passage are immune to the disturbance in the wave signals induced by the passing train, and therefore this set of indices can be readily applied to the monitoring of the health status of rail tracks.

## 5. Conclusions

Targeting structural health monitoring for railway tracks in HSR, a dedicated SHM framework which makes use of the sensitivity of DUWs is developed, supplemented by a benchmark-free condition contrast algorithm. In this framework, DUWs are generated and acquired with a sparse sensor network configured with only a pair of PZT-based sensing units. Based on the fact that the contacting status of the fatigue crack can be alternated by a load, DUW signals in a railway track are captured under different conditions (on-load and load-free), from which the discrepancies under different conditions are contrasted, and a set of damage indices is accordingly constructed. These DIs have proven effectiveness in quantitatively evaluating the accumulative severity and progress of a fatigue crack in the track. An all-in-one online diagnosis system is also developed, via which the proposed SHM framework is deployed and

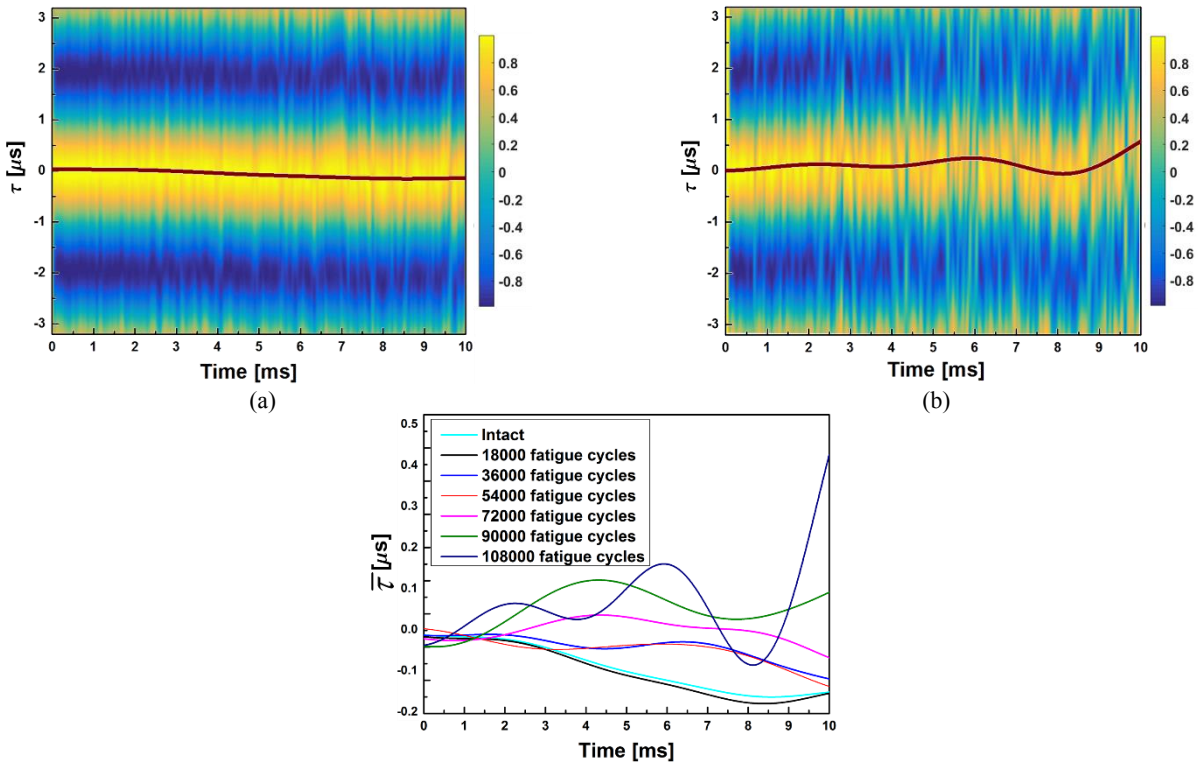


Fig. 15 Exemplary LCC ascertained when the railway track undergone (a) 18,000 and (b) 108,000 fatigue cycles; and (c) extracted

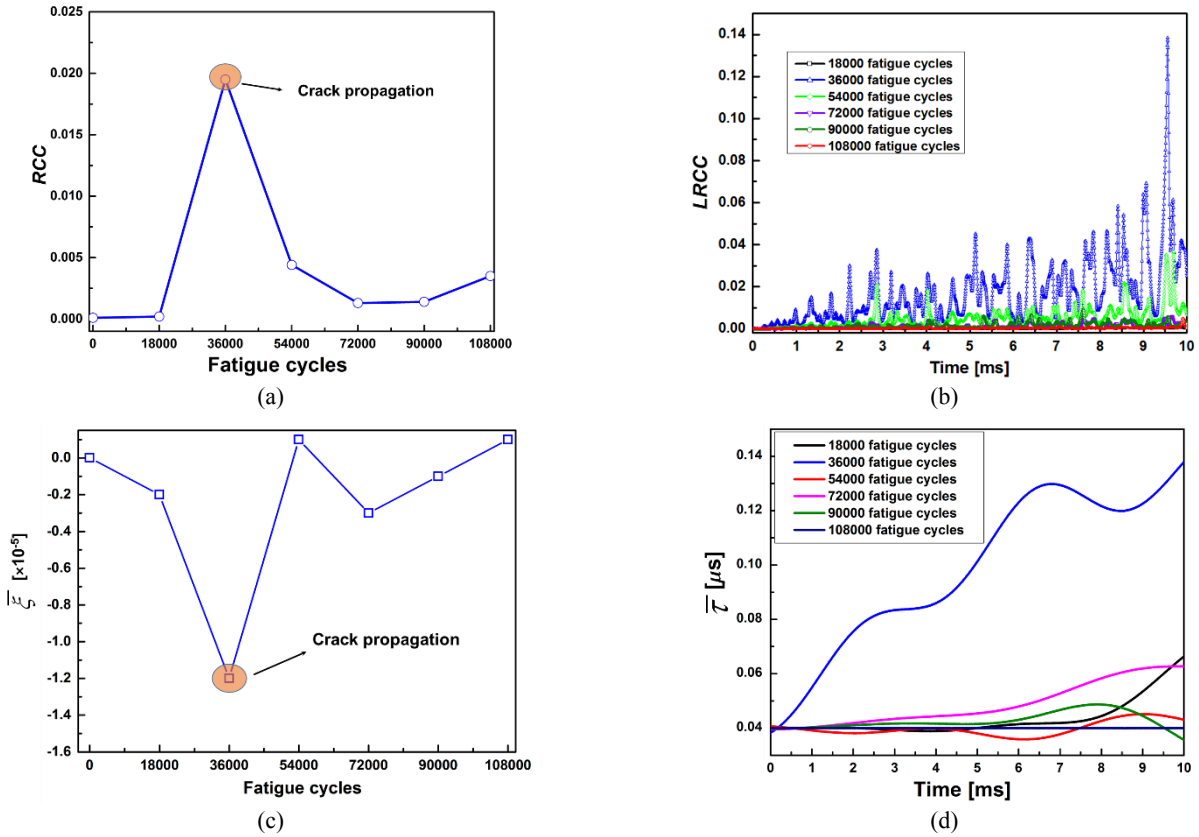


Fig. 16 Proposed DIs constructed using the signals from pre-load condition and the post-unload condition: (a) RCC; (b) LRCC; (c) $\bar{\xi}$; (d) $\bar{\tau}$

experimentally validated. A series of conformance tests is implemented, in which the health monitoring of a railway track obtained from China's HSR is performed. This method is capable of not only identifying the individual crack propagation, but also achieving an evaluation of the severity of the accumulated fatigue damage during the service lifetime. Endowed by the appealing merits of the diffuse features of DUWs compared with conventional GUWs, the proposed DUW-driven SHM has proven capability of monitoring the overall health of railway tracks in a highly cost-effective manner, while to some extent circumvent the restriction such as transducer installation onto railway tracks. Most importantly, instead of exploring the deviation from baseline signals obtained from intact specimen in conventional methods, the benchmark-free condition contrast algorithm enhances the practicability, robustness, and tolerance to ambient fluctuation of the SHM approach when applied to real-world HSR industry, warranting the performance of the system in adverse service conditions.

## Acknowledgments

The work was supported by a General Project (No. 51875492) and a Key Project (No. 51635008) received from the National Natural Science Foundation of China. The authors acknowledge the support from the Hong Kong Research Grants Council via General Research Funds (Nos.: 15201416 and 15212417). Z. Su thanks the National Rail Transit Electrification and Automation Engineering Technology Research Center for a research grant (No. BBY8).

## References

Adams, D.E. (2007), *Health Monitoring of Structural Materials and Components*: *Methods with Applications*, Hoboken: John Wiley & Sons, Ltd.

Adler, P.H., Olson, G.B. and Owen, W.S. (1986), "Strain hardening of Hadfield manganese steel", *Metallurg. Mater. Transact. A*, **17**, 1725-1737. https://doi.org/10.1007/BF02817271

Anugonda, P., Wiehn, J.S. and Turner, J.A. (2001), "Diffusion of ultrasound in concrete", *Ultrasonics*, **39**, 429-435. https://doi.org/10.1016/S0041-624X(01)00077-4

Bao, P., Yuan, M., Dong, S., Song, H. and Xue, J. (2013), "Fiber Bragg grating sensor fatigue crack real-time monitoring based on spectrum cross-correlation analysis", *J. Sound Vib.*, **332**, 43-57. https://doi.org/10.1016/j.jsv.2012.07.049

Bartoli, I., di Scalea, F.L., Fateh, M. and Viola, E. (2005), "Modeling guided wave propagation with application to the long-range defect detection in railroad tracks", *Ndt E Int.*, **38**, 325-334. https://doi.org/10.1016/j.ndteint.2004.10.008

BBC News, Ed. (2016), "India Train Crash: 115 Killed in Derailment near Kanpur."

Buck, O., Thompson, R.B. and Rehbein, D.K. (1988), "Ultrasonic measurements of crack tip shielding by closure", *Mater. Sci. Eng.*: *A*, **103**, 37-42. https://doi.org/10.1016/0025-5416(88)90549-6

Cawley, P., Lowe, M.J.S., Alleyne, D.N., Pavlakovic, B. and Wilcox, P. (2003), "Practical long range guided wave inspection - Applications to pipes and rail", *Mater. Eval.*, **61**, 66-74.

Chen, X., Michaels, J.E., Lee, S.J. and Michaels, T.E. (2012), "Load-differential imaging for detection and localization of fatigue cracks using Lamb waves", *Ndt E Int.*, **51**, 142-149. https://doi.org/10.1016/j.ndteint.2012.05.006

Clark, R. (2004), "Rail flaw detection: overview and needs for future developments", *Ndt E Int.*, **37**, 111-118. https://doi.org/10.1016/j.ndteint.2003.06.002

Croxford, A.J., Cheng, J. and Potter, J.N. (2016), "Nonlinear phased array imaging", *Proceedings of Health Monitoring of Structural and Biological Systems 2016*, 98052B, Las Vegas, NV, USA, April. https://doi.org/10.1117/12.2224744

Gandhi, N., Michaels, J.E. and Lee, S.J. (2012), "Acoustoelastic Lamb wave propagation in biaxially stressed plates", *J. Acoust. Soc. Am.*, **132**, 1284-1293. https://doi.org/10.1121/1.4740491

Ghiasi, R. and Ghasemi, M.R. (2018), "Optimization-based method for structural damage detection with consideration of uncertainties-a comparative study", *Smart Struct. Syst.*, *Int. J.*, **22**(5), 561-574. https://doi.org/10.12989/sss.2018.22.5.561

Han, H., Lu, G., Cong, P., Zhang, Q. and Wu, G. (2014), "Development of novel rail non-destructive inspection technologies", *Sensors Transduc.*, **179**, 121.

He, W.Y., Zhu, S. and Ren, W.X. (2018), "Progressive damage detection of thin plate structures using wavelet finite element model updating", *Smart Struct. Syst.*, *Int. J.*, **22**(3), 277-290. https://doi.org/10.12989/sss.2018.22.3.277

Hilloulin, B., Zhang, Y., Abraham, O., Loukili, A., Grondin, F., Durand, O. and Tournat, V. (2014), "Small crack detection in cementitious materials using nonlinear coda wave modulation", *Ndt E Int.*, **68**, 98-104. https://doi.org/10.1016/j.ndteint.2014.08.010

Hong, M., Wang, Q., Su, Z. and Cheng, L. (2014), "In situ health monitoring for bogie systems of CRH380 train on Beijing–Shanghai high-speed railway", *Mech. Syst. Signal Process*, **45**, 378-395. https://doi.org/10.1016/j.ymssp.2013.11.017

Lanza di Scalea, F., Rizzo, P., Coccia, S., Bartoli, I., Fateh, M., Viola, E. and Pascale, G. (2005), "Non-contact ultrasonic inspection of rails and signal processing for automatic defect detection and classification", *Insight-Non-Destruct. Test. Condit. Monitor.*, **47**, 346-353. https://doi.org/10.1784/insi.47.6.346.66449

Larose, E., Planes, T., Rossetto, V. and Margerin, L. (2010), "Locating a small change in a multiple scattering environment", *Appl. Phys. Lett.*, **96**, 204101. https://doi.org/10.1063/1.3431269

Li, F., Meng, G., Kageyama, K., Su, Z. and Ye, L. (2009), "Optimal mother wavelet selection for lamb wave analyses", *J. Intel. Mater. Syst. Struct.*, **20**, 1147-1161. https://doi.org/10.1177/1045389X09102562

Liu, Z., Li, W., Xue, F., Xiafang, J., Bu, B. and Yi, Z. (2015), "Electromagnetic tomography rail defect inspection", *IEEE Trans. Magn.*, **51**, 1-7. https://doi.org/10.1109/TMAG.2015.2430283

Lobkis, O.I. and Weaver, R.L. (2003), "Coda-wave interferometry in finite solids: Recovery of P-to-S conversion rates in an elastodynamic billiard", *Phys. Rev. Lett.*, **90**, 254302. https://doi.org/10.1103/PhysRevLett.90.254302

Mair, C. and Fararooy, S. (1998), "Practice and potential of computer vision for railways", In: *IEE Seminar Condition Monitoring for Rail Transport Systems*, London, UK, November. https://doi.org/10.1049/ic:19980983

Mariani, S., Nguyen, T., Zhu, X. and Lanza di Scalea, F. (2017), "Field test performance of noncontact ultrasonic rail inspection system", *J. Transport. Eng.*, *Part A*: *Syst.*, **143**, 04017007. https://doi.org/10.1061/JTEPBS.0000026

Michaels, J.E. and Michaels, T.E. (2005), "Detection of structural damage from the local temporal coherence of diffuse ultrasonic signals", *IEEE Trans. Ultrason. Ferroelectr. Freq. Control*, **52**, 1769-1782. https://doi.org/10.1109/TUFFC.2005.1561631

Ohara, Y., Mihara, T., Sasaki, R., Ogata, T., Yamamoto, S., Kishimoto, Y. and Yamanaka, K. (2007), "Imaging of closed cracks using nonlinear response of elastic waves at subharmonic frequency", *Appl. Phys. Lett.*, **90**, 011902. https://doi.org/10.1063/1.2426891

Ohara, Y., Horinouchi, S., Hashimoto, M., Shintaku, Y. and Yamanaka, K. (2011), "Nonlinear ultrasonic imaging method for closed cracks using subtraction of responses at different external loads", *Ultrasonics*, **51**, 661-666. https://doi.org/10.1016/j.ultras.2010.12.010

Ph Papaelias, M., Roberts, C. and Davis, C.L. (2008), "A review on non-destructive evaluation of rails: State-of-the-art and future development", *Proceedings of the Institution of Mechanical Engineers*, *Part F*: *Journal of Rail and Rapid Transit*, **222**, 367-384. https://doi.org/10.1243/09544097JRRT209

Pippan, R. and Hohenwarter, A. (2017), "Fatigue crack closure: a review of the physical phenomena", *Fatigue Fract. Eng. Mater. Struct.*, **40**, 471-495. https://doi.org/10.1111/ffe.12578

Planès, T. and Larose, E. (2013), "A review of ultrasonic Coda Wave Interferometry in concrete", *Cement Concrete Res.*, **53**, 248-255. https://doi.org/10.1016/j.cemconres.2013.07.009

Rajamäki, J., Vippola, M., Nurmikolu, A. and Viitala, T. (2018), "Limitations of eddy current inspection in railway rail evaluation", *Proceedings of the Institution of Mechanical Engineers*, *Part F*: *Journal of Rail and Rapid Transit*, **232**, 121-129. https://doi.org/10.1016/j.cemconres.2013.07.009

Rao, J., Ratassepp, M. and Fan, Z. (2016), "Guided wave tomography based on full waveform inversion", *IEEE Trans. Ultrason. Ferroelectr. Freq. Control*, **63**, 737-745. https://doi.org/10.1109/TUFFC.2016.2536144

Santa-Aho, S., Sorsa, A., Nurmikolu, A. and Vippola, M. (2014), "Review of railway track applications of Barkhausen noise and other magnetic testing methods", *Insight - Non-Destruct. Test. Condit. Monitor.*, **56**, 657-663. https://doi.org/10.1784/insi.2014.56.12.657

Shen, Y. and Cesnik, C.E. (2018), "Local interaction simulation approach for efficient modeling of linear and nonlinear ultrasonic guided wave active sensing of complex structures", *J. Nondest. Eval.*, **1**(1). https://doi.org/10.1115/1.4037545

Song, Z., Yamada, T., Shitara, H. and Takemura, Y. (2011), "Detection of damage and crack in railhead by using eddy current testing", *J. Electromagn. Anal. Applicat.*, **3**, 546. https://doi.org/10.4236/jemaa.2011.312082

Su, Z., Zhou, C., Hong, M., Cheng, L., Wang, Q. and Qing, X. (2014), "Acousto-ultrasonics-based fatigue damage characterization: Linear versus nonlinear signal features", *Mech. Syst. Signal Process*, **45**, 225-239. https://doi.org/10.1016/j.ymssp.2013.10.017

Thakkar, N.A., Steel, J.A., Reuben, R.L., Knabe, G., Dixon, D. and Shanks, R.L. (2006), "Monitoring of rail-wheel interaction using acoustic emission (AE)", *Adv. Mater. Res.*, **13**, 161-168. https://doi.org/10.4028/www.scientific.net/AMR.13-14.161

Wang, Q., Yuan, S., Hong, M. and Su, Z. (2015), "On time reversal-based signal enhancement for active lamb wave-based damage identification", *Smart Struct. Syst.*, *Int. J.*, **15**(6), 1463-1479. https://doi.org/10.12989/sss.2015.15.6.1463

Wang, J., Liu, X.Z. and Ni, Y.Q. (2018), "A Bayesian probabilistic approach for acoustic emission-based rail condition assessment", *Comput.-Aided Civil Inform.*, **33**, 21-34. https://doi.org/10.1111/mice.12316

Wang, K., Li, Y., Su, Z., Guan, R., Lu, Y. and Yuan, S. (2019a), "Nonlinear aspects of "breathing" crack-disturbed plate waves: 3-D analytical modeling with experimental validation", *Int. J. Mech. Sci.*, **159**, 140-150. https://doi.org/10.1016/j.ijmecsci.2019.05.036

Wang, N.B., Ren, W.X. and Huang, T.L. (2019b), "Baseline-free damage detection method for beam structures based on an actual influence line", *Smart Struct. Syst.*, *Int. J.*, **24**(4), 475-490. https://doi.org/10.12989/sss.2019.24.4.475

Zhang, X., Feng, N., Wang, Y. and Shen, Y. (2015), "Acoustic emission detection of rail defect based on wavelet transform and Shannon entropy", *J. Sound Vib.*, **339**, 419-432. https://doi.org/10.1016/j.jsv.2014.11.021

Zhang, Y., Tournat, V., Abraham, O., Durand, O., Letourneur, S., Le Duff, A. and Lascoup, B. (2017), "Nonlinear coda wave interferometry for the global evaluation of damage levels in complex solids", *Ultrasonics*, **73**, 245-252. https://doi.org/10.1016/j.ultras.2016.09.015

Zhang, X., Hao, Q., Wang, K., Wang, Y., Shen, Y. and Hu, H. (2018a), "An investigation on acoustic emission detection of rail crack in actual application by chaos theory with improved feature detection method", *J. Sound Vib.*, **436**, 165-182. https://doi.org/10.1016/j.jsv.2018.09.014

Zhang, Y., Larose, E., Moreau, L. and d'Ozouville, G. (2018b), "Three-dimensional in-situ imaging of cracks in concrete using diffuse ultrasound", *Struct. Health Monit.*, **17**, 279-284. https://doi.org/10.1177/1475921717690938

Zuo, P., Zhou, Y. and Fan, Z. (2016), "Numerical studies of nonlinear ultrasonic guided waves in uniform waveguides with arbitrary cross sections", *AIP Advances*, **6**, 075207. https://doi.org/10.1063/1.4959005

*HJ*